Polymer Degradation and Stability 248 (2026) 112059

Contents lists available at ScienceDirect

Polymer Degradation and Stability

journal homepage: www.journals.elsevier.com/polymer-degradation-and-stability

Phosphorus- nitrogen- and sulfur (P/N/S)-containing oligomer for enhanced flame retardancy of cotton

Jenny Alongi [a], Francesca Vasile [a], Federico Carosio [b], Matteo Arioli [a], Domenico Albanese [a], Elisabetta Ranucci [a,*]

[a] Dipartimento di Chimica, Università degli Studi di Milano, Via C. Golgi 19, 20133 Milan, Italy
[b] Dipartimento di Scienza Applicata e Tecnologia, Politecnico di Torino, Alessandria campus, Via T. Michel 5, 15121 Alessandria, Italy

ARTICLE INFO

Keywords:
P/N/S-containing polymers
Flame retardants
Functional coatings
Cotton

ABSTRACT

A phosphorus- nitrogen- and sulfur (P/N/S)-containing oligomeric flame retardant for cotton, designated DVP-CYSS, was synthesized via the polyaddition of divinyl ethylphosphinate with cystamine. Each repeat unit incorporates a disulfide linkage, two amine groups, and a phosphinate group. This molecular design aimed to evaluate whether integrating functionalities known to promote char formation in cotton into a single polymeric repeat unit could generate synergistic effects and thereby enhance flame retardant performance. Field Emission-Scanning Electron Microscopy observations indicated that the mechanical integrity of the cotton fibers is largely preserved upon deposition of DVP-CYSS at a 12.0% add-on. The flame retardant performance of DVP-CYSS was evaluated using multiple combustion tests, with M-CYSS, a disulfide-containing polyamidoamine lacking phosphorus groups, used as a benchmark. In vertical flame spread tests, DVP-CYSS outperformed M-CYSS, achieving higher efficacy and completely suppressing afterglow at add-ons between 8.0% and 16.0%. In horizontal flame spread tests, DVP-CYSS inhibited cotton combustion at a 10.0% add-on, whereas M-CYSS underwent thermo-oxidation for approximately 60 s. Oxygen-consumption cone calorimetry showed that DVP-CYSS reduced the peak heat release rate of cotton by 24% and the total smoke release by 65%, while yielding a 9% residual mass, in contrast to the negligible residue observed for untreated cotton. Elemental analysis of chars by Energy Dispersive Spectroscopy showed that, while sulfur content decreased, likely due to S–S bond cleavage followed by oxidation and volatilization, phosphorus remained largely in the char, likely contributing to its action in the condensed phase.

1. Introduction

The demand for efficient and environmentally sustainable flame retardants (FRs) has significantly increased in recent years due to growing restrictions on halogenated systems and concerns about their toxicity and persistence in the environment [1,2]. In this context, polymers and additives containing phosphorus (P), nitrogen (N), and sulfur (S) have emerged as promising alternatives, offering multifunctional flame retardant mechanisms and synergistic effects that act both in the condensed and gas phases.

Phosphorus-based moieties are well recognized for their ability to promote char formation and stabilize the condensed phase [3,4]. During combustion, phosphorus species catalyze dehydration and cross-linking reactions, leading to the formation of a coherent and insulating char layer that slows heat, oxygen and mass transfer [5–7]. Nitrogen functionalities enhance the release of flame-diluting nitrogen-containing gases such as NH_3 during degradation, which dilute flammable volatiles and oxygen in the flame zone while improving char cohesion [8]. Sulfur-containing groups, primarily acting through gas-phase radical scavenging [9], generate species such as SO_2 and thiyl radicals upon thermal decomposition. These species suppress flame-propagating radicals, thereby interrupting combustion, and are also believed to promote cross-linking reactions that strengthen the condensed-phase char [10].

The incorporation of P, N, and S within a single polymer framework produces notable synergistic effects [11–16]. In a previous study, a P/S/N-based polyamidoamine PAA) incorporating a disulfide group and two phosphonate groups per repeat unit was synthesized via the reaction of N,N′-methylenebisacrylamide with tetraethyl(((disulfanediylbis (ethane-2,1-diyl))bis(azanediyl))bis(ethane-2,1-diyl))bis(phosphonate)

* Corresponding author at: Dipartimento di Chimica, Università degli Studi di Milano, via C. Golgi 19, 20133 Milano, Italy,
E-mail address: elisabetta.ranucci@unimi.it (E. Ranucci).

https://doi.org/10.1016/j.polymdegradstab.2026.112059
Received 17 February 2026; Received in revised form 10 March 2026; Accepted 11 March 2026
Available online 11 March 2026

[17]. This PAA outperformed a reference N/S disulfide-containing PAA, prepared from N,N′-methylenebisacrylamide and cystine, coded M-CYSS [18,19], in horizontal flame spread tests, and in smoke suppression and total gas release reduction. These results motivated the design of a new cystine-based P/N/S flame retardant, designated DVP-CYSS, obtained from the polyaddition of cystamine with divinyl ethylphosphinate, which was previously shown to react under mild conditions with primary amines [20]. Its flame retardant performance on cotton was compared to that of the P-deprived PAA, M-CYSS, which had previously shown flame suppression in vertical tests but required add-ons ≥16.0%. Both DVP-CYSS and M-CYSS contain a disulfide group per repeat unit; however, DVP-CYSS additionally bears a phosphinate group, whereas M-CYSS has two carboxylate groups. Consequently, M-CYSS serves as a useful benchmark for evaluating the effectiveness of incorporating phosphinate groups into PAA repeat units to enhance flame retardancy. Notably, dialkyl phosphinates with short alkyl chains exhibit hydrophobic character, high thermal stability (>350 °C), and excellent flame retardant performance [3,21–25]. In addition, diethyl vinylphosphinate has been shown to confer flame retardancy when incorporated via radical copolymerization with styrene, methyl methacrylate, acrylonitrile, and acrylamide [26,27].

These premises highlight the strong potential of DVP-CYSS as halogen-free flame retardant for cotton in applications demanding smoke suppression, low gas emission, and high material performance.

2. Materials and methods

2.1. Materials

Cystamine (>98%), triethylamine (>99%), diethyl ether, dichloromethane, anhydrous sodium sulfate, deuterium oxide (D_2O, >99%), vinyl magnesium bromide (1 M THF solution), ethyl dichlorophosphinate (>96%) were supplied by Sigma-Aldrich (Milan, Italy). Cotton (COT) with an area density of 240 g•m^{-2} was purchased from Fratelli Ballesio S.r.l. (Turin, Italy).

2.2. Synthesis of ethyl divinylphosphinate

In a three necked flask equipped with an addition funnel, thermometer, and nitrogen inlet, a 1 M THF solution of vinyl magnesium bromide (60 mL) was added dropwise to a stirred solution of ethyl dichlorophosphinate (4.89 g, 30 mmol) in THF at – 78 °C in an acetone/dry ice bath.

The resulting solution was kept at – 78 °C for 1 h and quenched by addition of EtOH (10 mL). The reaction mixture was gradually returned to room temperature and the solvent evaporated under reduced pressure. The residue was purified through flash chromatography on silica gel using DCM/EtOH (97/3) as eluent providing the title compound (3.42 g, 23.4 mmol) in 78% yield.

The compound was found to be stable when dissolved in D_2O at room temperature for 4 days. The ^{1}H-NMR and ^{31}P- NMR spectra are reported in Figure S1a and S1b, respectively, in Supplementary Materials.

2.3. Synthesis of DVP-CYSS

In a screw cap vial ethyl divinylphosphinate (1.00 g, 6.84 mmol) was dissolved in water (0.5 mL). Cystamine (6.84 mmol, 1.04 g) was weighed in a separate vial, dissolved in water (0.5 mL) and transferred to the vial containing divinylphosphinate. Additional water (1.3 mL) was used to wash residues of cystamine and added as well to the vial in order to maintain the desired 1:1 stoichiometric ratio. The reaction was stirred at 25 °C in the dark for 96 h. The crude was thus transferred into a one necked flask to evaporate water at reduced pressure to generate a viscous yellow syrup 1.99 g, 98% yield.

2.4. Synthesis of M-CYSS

M-CYSS was synthesized following the procedure previously reported [28]. Briefly, *N,N'*-methylenebisacrylamide (1.55 g, 10.00 mmol), L-cystine (2.41 g, 10.00 mmol) and lithium hydroxide monohydrate (0.86 g, 20.00 mmol) were dissolved in H_2O (4 mL), heated under stirring to 50 °C until the complete dissolution of monomers. The reaction mixture was cooled to 25 °C and left at this temperature in the dark for 2 days. Afterward, it was diluted to 10 mL with water, and the pH was adjusted to 8.5 using a 1 M HCl solution. The product was finally isolated by freeze-drying, affording a nearly quantitative yield.

2.5. Treatment of cotton fabrics with DVP-CYSS and M-CYSS

Strips of cotton fabric, cut to specific sizes according to the mechanical and combustion test requirements (see Sections 2.7 *Characterization methods and 2.8 Combustion tests of DVP-CYSS-treated cotton fabrics*), were dried at 100 °C for 2 min and subsequently weighed. Samples were then impregnated with aqueous solutions of DVP-CYSS or M-CYSS of suitable concentration, drying at 100 °C for 2 min. The concentrations of the impregnating solutions and the final add-ons were: 8.0, 10.0, 12.0 and 16.0% for depositing 8.0, 10.0, 12.0 and 16.0% add-on.

The total dry solid add-ons (Add-on %) were determined by weighing each sample before (W_i) and after drying following impregnation (W_f). The add-ons were calculated according to Eq. (1):

$$Add-on\ \% = \frac{W_f - W_i}{W_i} \times 100 \quad \text{(Eq. 1)}$$

Treated-cotton fabrics were coded with the prefix COT/ followed by the code of the DVP-CYSS or M-CYSS employed. Therefore, COT/ DVP-CYSS and COT/M-CYSS stands for cotton samples treated with DVP-CYSS and M-CYSS, respectively.

2.6. Thermo-oxidation of COT/DVP-CYSS fabrics

COT/DVP-CYSS samples (30 mm × 60 mm each) were placed in porcelain crucibles and heated in air using a 21HT Fratelli Galli oven (Fizzonasco, Italy) at a rate of 10 °C min^{-1} up to 350 °C. Samples were held at this temperature for 2 min before being transferred to open air.

2.7. Characterization methods

2.7.1. NMR analyses

NMR (Nuclear Magnetic Resonance) analyses of divinylphosphinate and DVP-CYSS were performed in D_2O and $CDCl_3$. All spectra were acquired on a Bruker Avance 600 MHz spectrometer operating at 298 K. One-dimensional ^{1}H and ^{31}P spectra, as well as two-dimensional ^{1}H–^{13}C HSQC (Heteronuclear Single Quantum Coherence), HMBC (Heteronuclear Multiple Bond Correlation), and ^{1}H–^{15}N HMBC experiments, were recorded for structural characterization.

For ^{31}P NMR experiments, a spectral width of 300 ppm (from −150 to +150 ppm) was used, with a relaxation delay of 10 s. ^{15}N experiments were acquired using a spectral width of 160 ppm (from −10 to +150 ppm). Water suppression was achieved using the excitation sculpting technique.

^{1}H DOSY (Diffusion-Ordered SpectroscopY) NMR experiments were carried out using a 2D DOSY pulse sequence from the standard Bruker library, employing a stimulated echo sequence with bipolar gradient pulses for diffusion and excitation sculpting with gradients for water suppression. The diffusion delay (Δ) was set to 150 ms, and the gradient pulse duration (δ) was 1 ms. Also, ^{31}P DOSY NMR spectrum was acquired using 2D DOSY pulse sequence from the standard Bruker library, employing a stimulated echo sequence and INEPT for polarization transfer. DOSY data were processed using the standard Bruker Dynamic Center procedure.

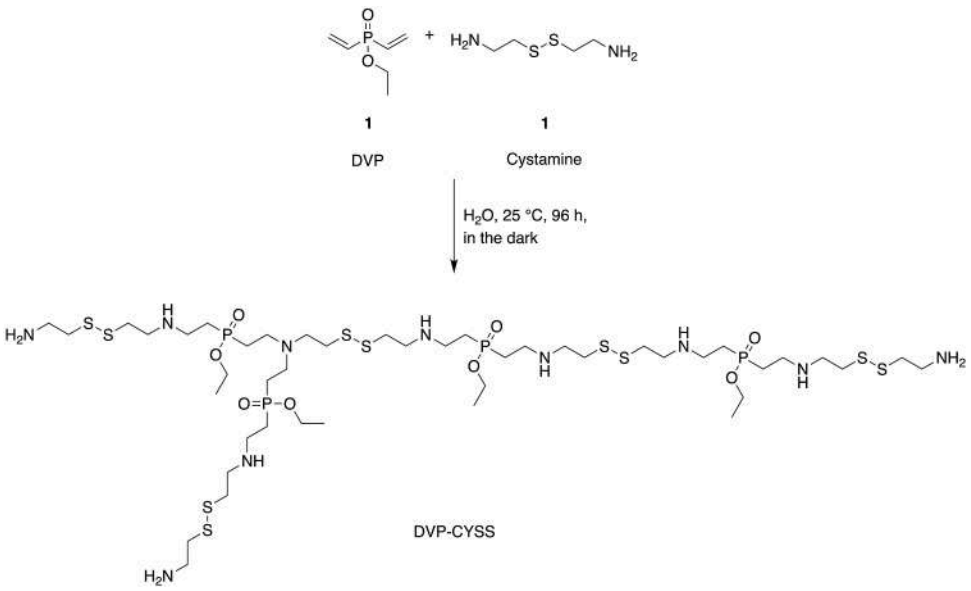

Scheme 1. Synthesis of DVP-CYSS.

2.7.2. Whiteness index

The whiteness index (WI) was determined on 30 mm x 60 mm specimens, according to the ISO 2469 standard [29], using a SA0835/OWM SAMA whiteness meter (SAMA Tools, Viareggio, Italy). each measurement was repeated ten times, and the mean value was reported together with the corresponding standard deviation (σ) as experimental error.

2.7.3. Thermogravimetric analysis

Thermogravimetric analysis (TGA) of untreated cotton (COT) and DVP-CYSS- and M-CYSS treated cotton fabrics (COT/DVP-CYSS and COT/M-CYSS, respectively) was carried out under inert (N_2) and oxidative (air) atmospheres using a TA Q500 analyser (TA Waters, Milan, Italy) with a gas flow of 20 mL min^{-1}. Measurements were performed from 50 to 800 °C at a heating rate of 10 °C min^{-1} on samples (~5 mg) placed in open alumina crucibles.

2.7.4. Scanning electron microscopy

Surface morphology was observed by field-emission scanning electron microscopy (FE-SEM, ZEISS SIGMA 300, Zeiss, Ramsey, NJ, USA) operated at 5 kV accelerating voltage and 8.5 mm working distance after platinum sputter-coating. Elemental analysis was assessed by energy-dispersive X-ray spectroscopy (EDS) using scanning electron microscope (ZEISS EVO 15, Zeiss, Ramsey, NJ, USA) equipped with an Oxford Instruments Ultim Max 40 detector (Jena, Germany). Fabric samples (5 mm × 5 mm) were mounted on aluminium stubs and sputter-coated with platinum prior to analysis. The elemental composition determined by EDS was obtained as the average of five independent measurements.

2.7.5. Mechanical testing

Tensile tests were performed on cotton specimens 15 mm x 100 mm in length according to the ISO13934 standard [30]. Analyses were performed using an Instron 5966 (Instron, High Wycombe, UK) instrument equipped with wave clamps; setting: 10 mm min^{-1} strain rate, and 2 N preload. The test was repeated on 10 specimens. The values of Young's modulus, force at break, and elongation at break (%) are reported as the mean ± standard deviation (σ) of these tests.

2.7.6. Combustion tests of DVP-CYSS-treated cotton fabrics

Horizontal flame spread tests (HFSTs) and Vertical flame spread tests (VFSTs) were carried out by applying a 20 ± 5 mm long butane flame to the short edge of 30 mm × 60 mm specimens according to the ISO 3795 [31] and ISO 15025 [32] standards, modified in terms of cotton size specimens and flame application time. In the horizontal configuration, each specimen was positioned on a metallic frame tilted at a 45° angle of along its longitudinal axis and then ignited for 3 s. In the vertical configuration, the butane flame was applied for 2 s to the center of the short edge of the specimens. All combustion tests were tripled and the total combustion time (s) and residual mass fraction (RMF, %) were determined.

The resistance of square fabric samples (100 mm × 100 mm) to a 35 kW•m^{-2} irradiative heat flux was investigated using an oxygen-consuming cone calorimeter (Nose-lab ATS advanced, Milan, Italy). Measurements were performed in the horizontal configuration according to a previously reported procedure [33], optimized based on the ISO 5660 standard [34]. Parameters such as the time to ignition (TTI, s), time to flameout (TTF, s), heat release rate peak (pkHRR, kW•m^{-2}), total heat release (THR, MJ•m^{-2}), total smoke release during non-flaming phase ($TSR_{(NFP),}$ m^2 m^{-2}), total smoke release during flaming phase ($TSR_{(FP),}$ m^2 m^{-2}), and residual mass fraction (RMF, wt.%) were determined. Each test was performed in triplicate, and the standard deviation was calculated.

Prior to the combustion tests, all specimens were conditioned to constant weight in a climatic chamber at 23 ± 1 °C and 50% relative humidity for 48 h.

3. Results and discussion

3.1. Synthesis and structural elucidation of DVP-CYSS

The P/N/S-containing oligomer coded DVP-CYSS was obtained by the aza-Michael polyaddition of cystamine with divinylphosphinate in a 1:1 molar ratio (Scheme 1). The 2:1 ratio of N–H to double-bond reactive functions in the monomer mixture suggests the formation of an oligomeric product, even though the four cystamine N–H groups are unlikely to be equally reactive, since the first addition converts a primary amine into a less reactive, sterically hindered secondary amine. Accordingly, complementary NMR techniques were used to determine the chemical structure of DVP-CYSS. Specifically, ^{1}H, ^{1}H–^{13}C HSQC, ^{31}P, and ^{1}H–^{15}N HMBC spectra were acquired.

In the ^{1}H and ^{1}H–^{13}C HSQC spectra (Fig. 1a and b), the signals of the ethyl groups are clearly identifiable at 1.26/16.2 ppm and 4.04/61.6 ppm, respectively. The signals of the CH_2 protons α to the ^{31}P appear in

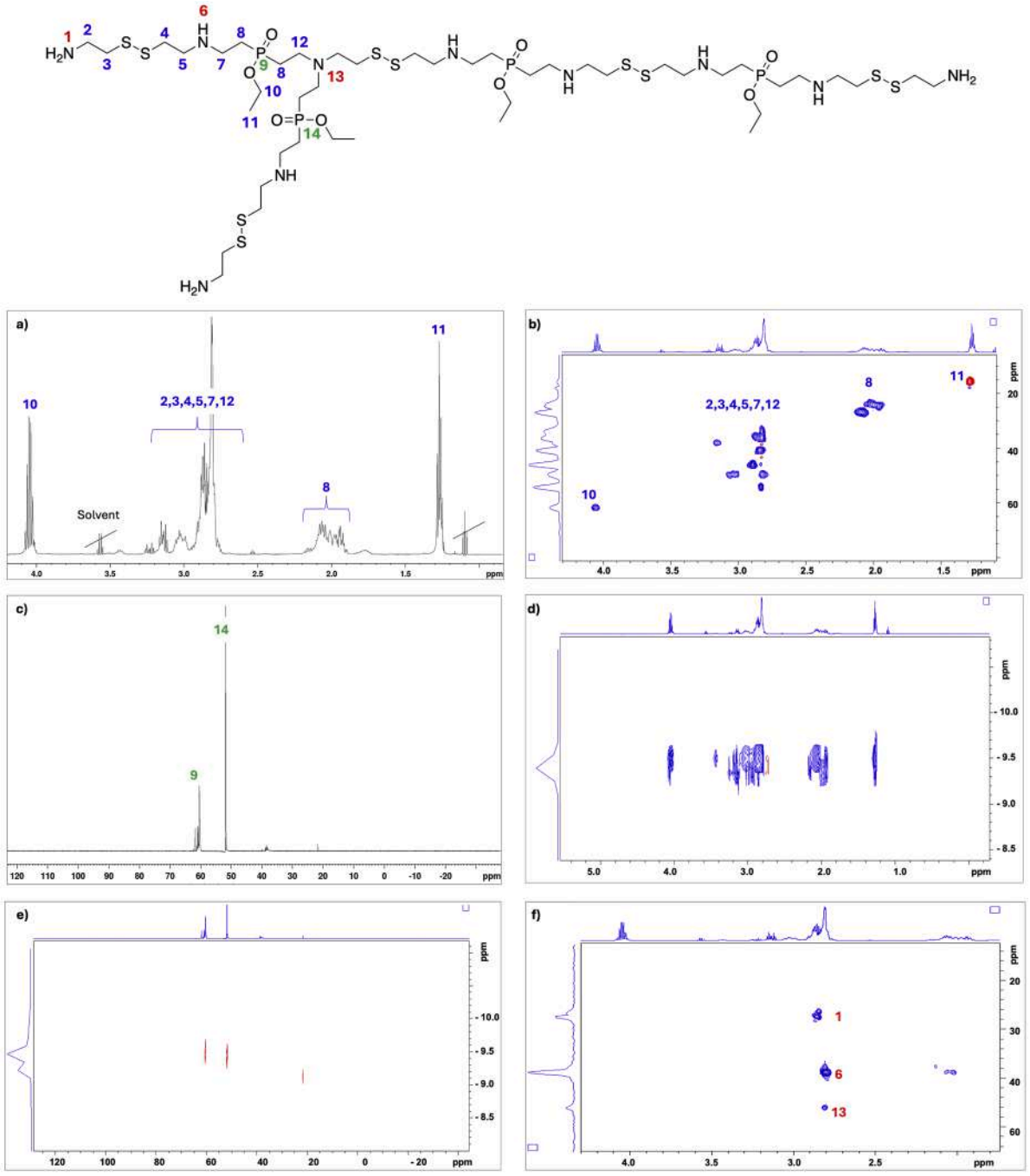

Fig. 1. ^{1}H NMR (a), ^{1}H–^{13}C HSQC (b), ^{31}P NMR (c) spectra of DVP-CYSS. ^{1}H–^{13}C HSQC spectrum shows one-bond correlations between proton and carbon nuclei. ^{1}H DOSY NMR spectrum (d) of DVP-CYSS recorded using a stimulated echo pulse sequence with bipolar gradient pulses. ^{31}P DOSY NMR (e) spectrum of DVP-CYSS recorded using a stimulated echo pulse sequence with INEPT for non-selective polarization transfer and decoupling during acquisition. ^{1}H–^{15}N HMBC spectrum (f) of DVP-CYSS, showing long-range correlations between proton and nitrogen nuclei. All spectra were recorded in D_2O at 25 °C on a Bruker Avance 600 MHz spectrometer.

the range 1.9–2.1 ppm, with ^{13}C chemical shifts at 23.5 and 27 ppm. The nitrogen-bound CH_2 protons are observed between 2.77 and 3.16 ppm, with ^{13}C chemical shifts between 32.6 and 54.5 ppm. The ^{1}H spectrum shows good resolution, without line broadening typically observed for high-molecular-weight polymers due to shorter T_2 relaxation time and free induction decay. Notably, the ^{31}P spectrum displays two sets of signals at 60.5 and 51.8 ppm in a 1:1 integral ratio, suggesting the presence of two different phosphorus species in the molecule (Fig. 1c).

DOSY spectra enabled estimation of the molecular size of DVP-CYSS from the measured diffusion coefficient (D), using the empirical relationship $D = K \cdot Mw^{-0.49}$, which is applicable for water soluble macromolecules [35]. The K coefficient was estimated as 1.05×10^{-8} m^2 s^{-1} from a calibration curve ranging from the monomer to polylactic acid polymers up to 49000 Da. DOSY spectra were recorded for both ^{1}H (Fig. 1d) and ^{31}P nuclei (Fig. 1e). The diffusion coefficient of DVP-CYSS was measured as $D = 3.16 \times 10^{-10}$ m^2 s^{-1}, while divinyl ethyl phosphinate showed a significantly higher diffusion coefficient ($D = 9.13 \times 10^{-10}$ m^2 s^{-1}). Application of the above empirical correlation yielded an estimated molecular weight of approximately 1270, indicating a low polymerization degree.

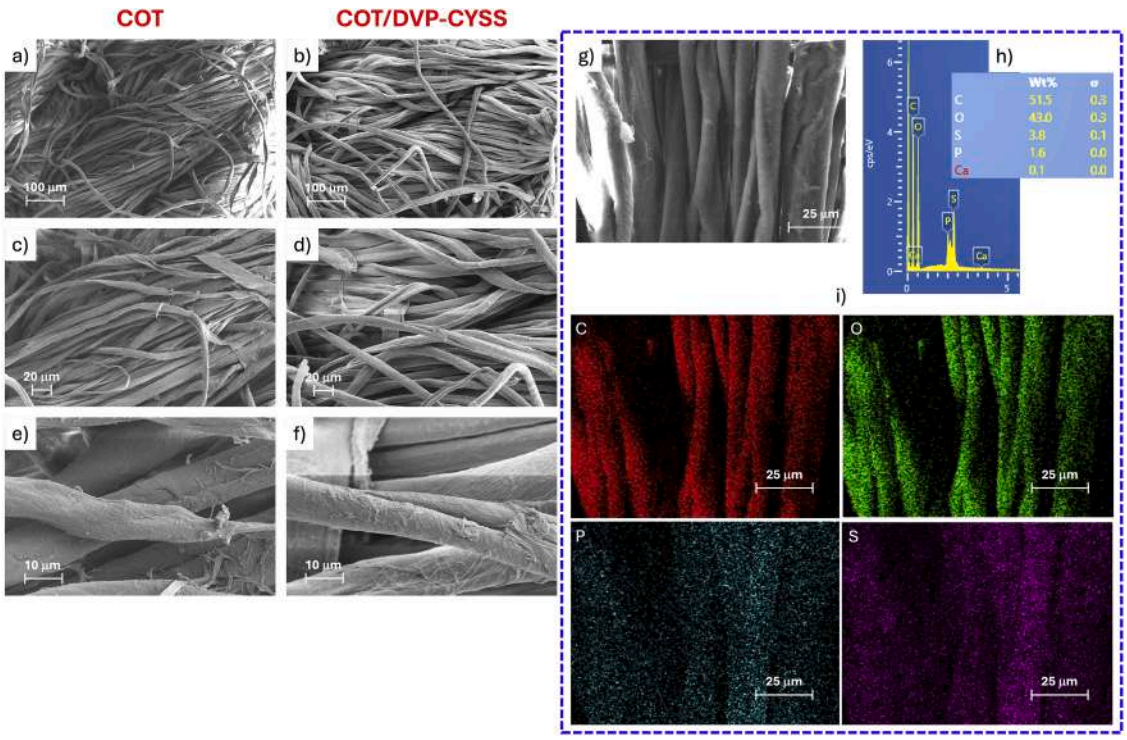

Fig. 2. SEM magnifications of untreated cotton (COT, a, c and e at 500x, 1000x and 5000x magnifications, respectively) and cotton treated with DVP-CYSS with a 12.0% add-on (COT/DVP-CYSS, b, d and f at 500x, 1000x and 5000x magnifications, respectively). SEM micrograph of COT/DVP-CYSS (g, at 2500x magnifications) with corresponding elemental analysis (h) and elemental maps of C (red), O (green), P (petrol blue), and S (purple) (i).

Further structural information was obtained from the $^{1}H–^{15}N$ HMBC spectrum (Fig. 1f), which revealed three distinct ^{15}N resonances at 27.3, 38.9, and 46.1 ppm, corresponding to primary, secondary, and tertiary amines, respectively. To obtain a semi-quantitative estimate of the relative amounts of these nitrogen environments, the ^{15}N projection of the HMBC spectrum was analyzed. Each ^{15}N signal gives rise to a set of cross-peaks with ^{1}H, and by integrating these signals, it is possible to estimate the relative distribution of the nitrogen atoms. Although this approach is not fully quantitative due to differences in magnetization transfer and relaxation times, it provides a reliable indication of relative abundances. Normalization of the integrated intensities yielded an approximate ratio of 3:6:1 for primary, secondary, and tertiary amines, respectively.

Combining the information from the ^{1}H-^{15}N HMBC and ^{31}P spectra, and ^{1}H integrations, a plausible structural hypothesis for the obtained oligomer is shown in Scheme 1. The tertiary nitrogen resonance points to a branched structure, but the specific site of branching along the main oligomer backbone could not be conclusively assigned. The observation of two sets of well-resolved ^{31}P NMR signals indicates the formation of structurally and conformationally distinct oligomers during the synthesis. All detected species are fully consistent with the NMR data and can be considered structurally correlated to the scaffold depicted in Fig. 1.

3.2. Morphological and mechanical characterization of DVP-CYSS-treated cotton fabrics

The morphology of COT/DVP-CYSS samples was observed by FE-SEM and compared with that of untreated cotton (Fig. 2a-f). Both untreated and treated fibers exhibited predominantly smooth surfaces. At higher magnification, a thin polymer coating was observed on the surface of COT/DVP-CYSS fibers (Fig. 2f). EDS analysis confirmed a homogeneous distribution of DVP-CYSS, as shown by the even distribution of carbon (C), oxygen (O), nitrogen (N), sulfur (S), and phosphorous (P) elements (Fig. 2g-i).

Table 1
Tensile stress-strain results of untreated and DVP-CYSS-treated and cotton samples.

Sample	Young's modulus ± σ (MPa)	Force at break ± σ (N)	Elongation at break % ± σ
COT	140.6 ± 5.06	223.6 ± 12.7	52.2 ± 1.59
COT/DVP-CYSS	143.8 ± 4.24	205.5 ± 10.8	47.8 ± 1.66

The FT-IR spectrum of COT/DVP-CYSS was essentially superimposable to that of pristine cotton (Fig. S2), likely due to the localization of the DVP-CYSS coating within the deeper layers of the cotton fibers.

Notably, the whiteness index of cotton showed a slight decrease after DVP-CYSS treatment, declining from 77.6 ± 0.53 to 74.4 ± 1.09.

The effect of the DVP-CYSS coating on the mechanical properties of cotton was evaluated through tensile tests performed on samples with a 12.0% add-on. Table 1 reports the tensile parameters observed, compared with those of pristine cotton. As shown, only negligible differences were detected, demonstrating that the mechanical response of cotton was not affected by the presence of DVP-CYSS.

3.3. Thermal characterization of DVP-CYSS-treated cotton fabrics

The thermal stability of untreated and DVP-CYSS-treated cotton fabrics was investigated by TGA under nitrogen and air in the 50-800 °C range (Fig. 3). The $T_{onset10\%}$, T_{max} and RMF values are reported in Table 2. In nitrogen (Fig. 3a), COT, COT/DVP-CYSS and COT/M-CYSS, where M-CYSS is the flame retardant benchmark used in this study, showed a single main weight loss event. Untreated cotton remained thermally stable up to 300 °C, with approximately 80% of the total weight loss occurring between 300 and 375 °C, as expected [36]. DVP-CYSS-treated cotton fabrics significantly anticipated cotton decomposition, as clearly demonstrated by the $T_{onset10\%}$ and T_{max} values (Table 2). However, compared with untreated cotton, the

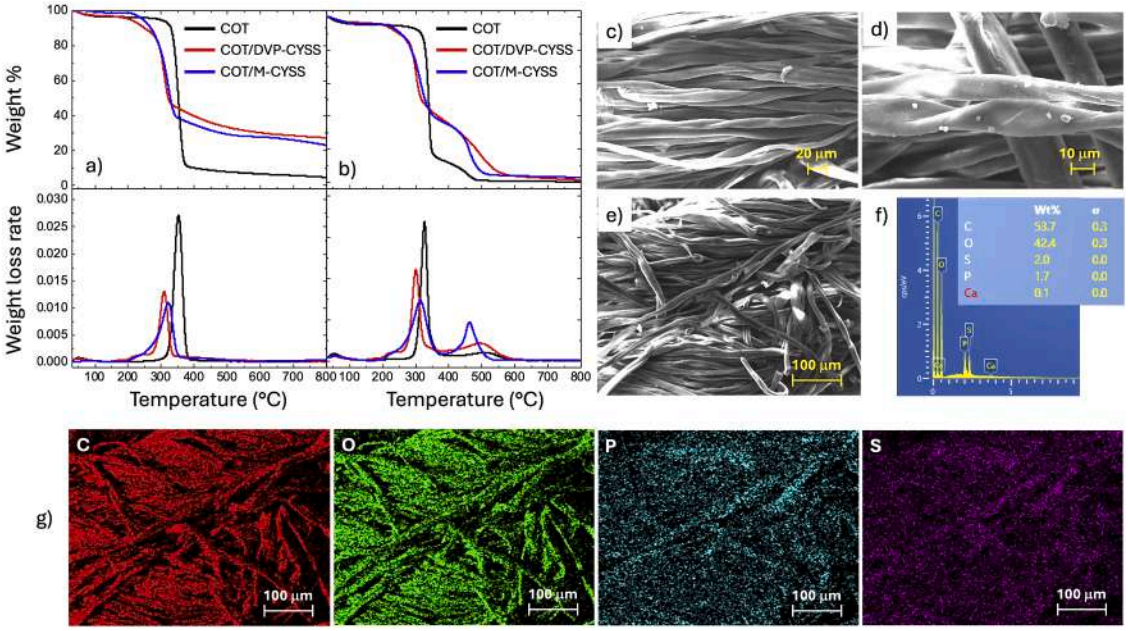

Fig. 3. TG and DTG thermograms of untreated cotton (COT) and cotton treated with DVP-CYSS (COT/DVP-CYSS, add-on: 12.0%) and M-CYSS (COT/M-CYSS add-on: 12.0%) under nitrogen (a) and air (b). SEM micrographs of the COT/DVP-CYSS residue at 300 °C (c-e, at 1000x, 2500x, and 500x magnifications, respectively), and EDS analysis (f) with elemental maps of C (red), O (green), P (petrol blue), and S (purple) (g).

Table 2
Thermal data of COT/ DVP-CYSS and COT/M-CYSS samples in nitrogen and air by thermogravimetric analysis.

Sample	$T_{onset10\%}$ (°C) [a]	T_{max1} (°C) [b]	T_{max2} (°C) [c]	RMF (%) [c]
Nitrogen				
COT	330	353	-	4.5
COT/DVP-CYSS	249	308	-	27.3
COT/M-CYSS	269	320	-	23.5
Air				
COT	317	327	509	0
COT/ DVP-CYSS	251	301	490	1.9
COT/M-CYSS	254	318	496	2.8

[a] Onset decomposition temperature at 10 % weight loss. [b] First temperature at maximum weight loss rate. [c] Second and third temperature at maximum weight loss rate. [d] Residual mass fraction at 800 °C.

COT/DVP-CYSS samples produced a significantly higher amount of thermally stable char above 300 °C, with RMF values remaining nearly constant up to 800 °C. This behavior closely resembles that observed for M-CYSS At 800 °C, the RMF values were indeed 27.5 and 23.5% for COT/DVP-CYSS and COT/M-CYSS, respectively, compared with only 4.5% for untreated cotton.

In air (Fig. 3b), the TG thermogram of untreated cotton displays two main weight-loss events, occurring between 300 and 375 °C and between 375 and 500 °C. Similar to its behavior in nitrogen (Table 2), untreated cotton remains thermally stable up to 300 °C, losing about 85% of its weight above this temperature. However, due to thermal oxidation, its RMF decreases to negligible levels as early as around 550 °C. In the cases of the DVPCYSS- and M-CYSS-treated cotton fabrics, the TG curves are almost superimposable up to 300 °C, but they differ significantly at higher temperatures. In fact, COT/DVP-CYSS undergoes a second decomposition step between 300 and 600 °C, characterized by a slow weight loss with a T_{max2} at 490 °C, while COT/M-CYSS rapidly decomposes in the 300-500 °C range, exhibiting its intrinsic intumescent behavior, as expected [18,19], with a T_{max2} at 496 °C.

A plausible hypothesis is that the oxidation behavior of COT/DVP-CYSS is influenced by DVP-CYSS promoting cotton dehydration, a process recognized as the prevailing char-forming mechanism [36], thereby inhibiting depolymerization. To test this hypothesis, COT/DVP-CYSS was subjected to thermo-oxidation by heating in air at 300 °C, and the morphology of the resulting oxidation product examined using FE-SEM (Fig. 3c and e) and EDS analysis with elemental mapping of C, O, P, and S (Fig. 3f and g). Comparison of the FE-SEM images of the thermo-oxidation residues of COT (Fig. 2) and COT/DVP-CYSS (Fig. 3) reveals that the native cotton texture is largely retained after oxidation, indicating that depolymerization plays a negligible role, as it normally results in fiber fibrillation. Elemental analysis confirmed the presence of P and S in the oxidized residue at 300 °C, in addition to C and O. Interestingly, although the C, O, and P contents remain nearly unchanged, the sulfur content decreases by approximately 50%. This observation may suggest that part of the S forms volatile sulfur-containing degradation products released into the gas phase, while P mainly remains in the condensed phase. Notably, unlike M-CYSS, no intumescence was observed, indicating that DVP-CYSS follows a distinct thermo-oxidative pathway.

3.4. Combustion tests of DVP-CYSS-treated cotton fabrics

The combustion behavior of COT/ DVP-CYSS was investigated by Vertical Flame Spread Tests (VFSTs), Horizontal Flame Spread Tests (HFSTs), and oxygen-consumption cone calorimetry tests. The results were compared not only with those of COT, but also of COT/M-CYSS, whose performance in this respect had already been studied [18].

3.4.1. Vertical Flame Spread Tests

In VFSTs, untreated cotton showed rapid burning behavior and completely decomposed, leaving no residues at the end of the test. (Fig. 4a). Cotton samples treated with M-CYSS and DVP-CYSS at different add-ons, namely, 8.0, 10.0, 12.0 and 16.0% were compared (Fig. 4b and c). Although a 16.0% add-on of M-CYSS was previously shown to inhibit cotton combustion and DVP-CYSS proved also effective, a marked divergence emerged at a 12.0% add-on: COT/DVP-CYSS prevented ignition, whereas COT/M-M-CYSS did not.

Add-ons lower than 12.0%, namely 10.0 and 8.0%, for COT/DVP-

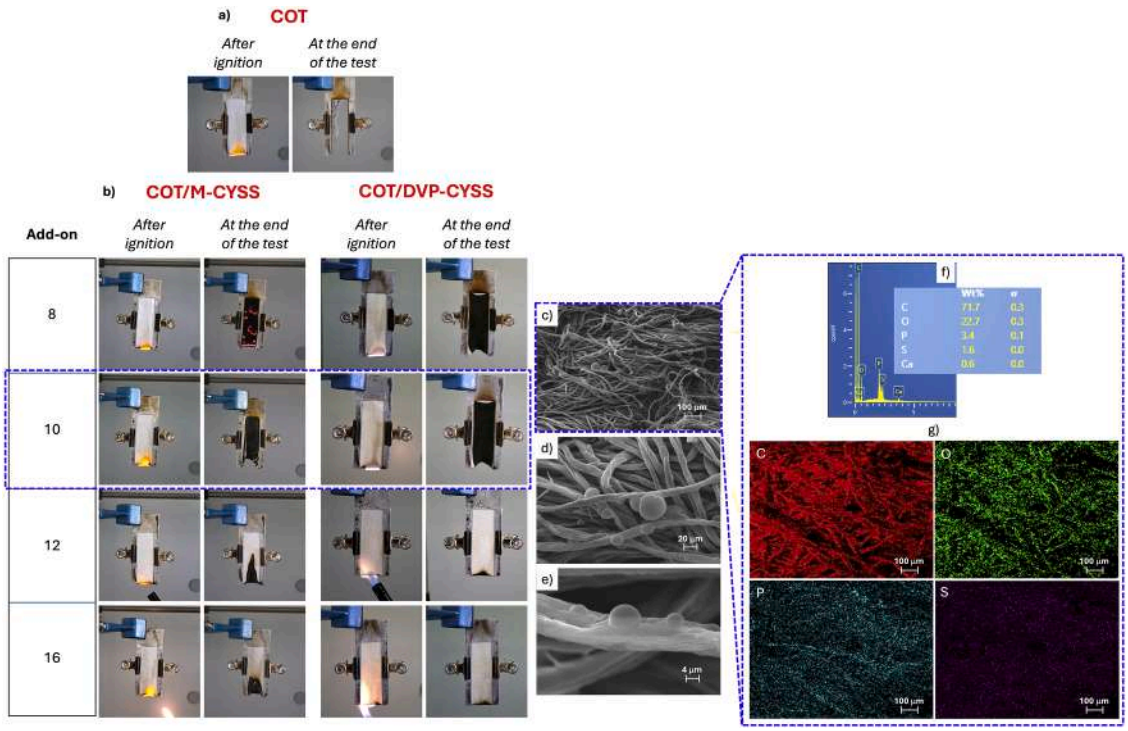

Fig. 4. Snapshots of vertical flame spread tests of untreated cotton (COT, a), and cotton treated with M-CYSS and DVP-CYSS at different add-ons (b). SEM micrographs of COT/DVP-CYSS with a 10.0% add-on (c, d and e, at 250x, 1000x and 5000x magnifications, respectively) with corresponding elemental analysis (f) and elemental maps of C (red), O (green), P (petrol blue), and S (purple) (g).

Table 3
Combustion data of untreated, DVP-CYSS and M-CYSS-treated cotton fabrics in VFSTs.

Sample	Add-on [(a)] (%)	Flaming combustion time [(b)] (s)	Afterglow (*combustion time, s*) [(c)] (s)	Extinguishment	RMF [(d)] (%)
COT	-	41	YES	NO	<1
COT/DVP-CYSS	16.0	0	NO	YES	100
COT/DVP-CYSS	12.0	0	NO	YES	100
COT/DVP-CYSS	10.0	15	NO	YES	65
COT/DVP-CYSS	8.0	17	NO	YES	58
COT/M-CYSS	16.0	1	YES (*100*)	YES	90
COT/M-CYSS	12.0	0	YES (*150*)	YES	80
COT/M-CYSS	10.0	7	YES (*223*)	NO	50
COT/M-CYSS	8.0	15	YES (*80*)	NO	30

[(a)] Add-on ± 0.5.0. [(b)] Combustion time ± 1 s. [(c)] Combustion time ± 1 s. [(d)] RMF ± 1.0%

CYSS showed comparable performances: the flame slid along the surface, reached the clamps in about 15 s, hence achieving the self-extinguishment, and left residues of 65 and 58% (Table 3), respectively, with no afterglow observed. Conversely, COT/M-CYSS at a 12.0% add-on achieved self-extinguishment but in exhibited a prolonged afterglow (150 s), while at 10.0 and 8.0% it did not self-extinguish, as the specimen was consumed by a long and persistent afterglow.

At the end of the tests, a COT/DVP-CYSS specimen with a 10.0% add-on was examined by FE-SEM. Similarly to the residue observed after thermo-oxidation at 300 °C (Fig. 3c, d and e), the fabric texture was preserved throughout (Fig. 4c, d and e); however, in this case, some bubbles were observed across the surface.

Regarding the elemental analysis of the residue left by COT/DVP-CYSS (add-on: 10.0%) after VFSTs, EDS analysis confirmed a homogeneous distribution of carbon (C), oxygen (O), nitrogen (N), sulfur (S), and phosphorous (P) elements, consistent with the chemical composition of DVP-CYSS (Fig. 4f and g).

3.4.2. Horizontal Flame Spread Tests

COT and COT/DVP-CYSS were tested in the horizontal configuration, and representative snapshots from the HFSTs are shown in Fig. 5. The main combustion parameters are summarized in Table 4. When exposed to the flame, untreated cotton burned slowly (53 s) and completely, leaving a residual mass fraction below 1%. In contrast, DVP-CYSS effectively inhibited cotton combustion at a 10.0% add-on, whereas M-CYSS underwent thermo-oxidation for approximately 60 s, as previously reported [18]. At the end of the tests, the residue from the COT/DVP-CYSS specimen was analyzed by FE-SEM. Consistent with observations after thermo-oxidation at 300 °C (Fig. 3c–e) and after VFSTs (Fig. 4c–e), the fabric texture remained largely intact (Fig. 5b–e). EDS analysis revealed a uniform distribution of carbon (C), oxygen (O), nitrogen (N), sulfur (S), and phosphorus (P), in agreement with the chemical composition of DVP-CYSS (Fig. 5f and g).

3.4.3. Oxygen-consumption cone calorimetry tests

COT/DVP-CYSS cotton samples were subjected to an irradiative heat flux of 35 $kW \bullet m^{-2}$ in an oxygen-consumption cone calorimeter and compared to untreated cotton. Combustion parameters including time to ignition (TTI), time to flameout (TTF), heat release rate peak (pKHRR),

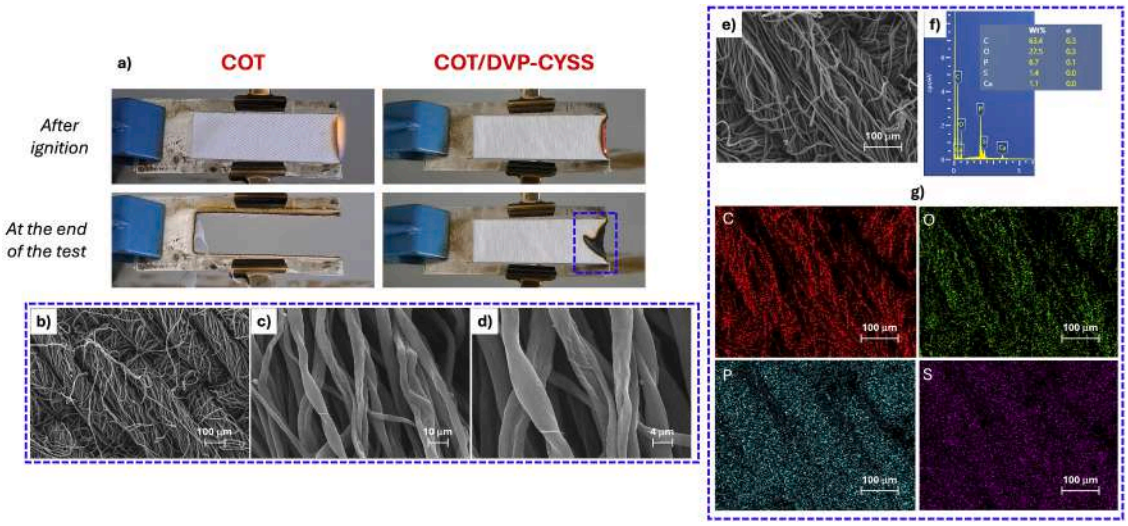

Fig. 5. Snapshots of horizontal flame spread tests for untreated cotton (COT) and cotton treated with DVP-CYSS (COT/ DVP-CYSS, add-on: 10.0%) (a). SEM micrographs of the COT/DVP-CYSS residue at the end of the test (b-d, at 250x, 2500x, and 5000x magnifications, respectively). SEM magnification (e, 250x) and EDS analysis (f) with elemental maps of C (red), O (green), P (petrol blue), and S (purple) (g).

Table 4
Combustion data of untreated, DVP-CYSS and M-CYSS-treated cotton fabrics in HFSTs.

Sample	Add-on [a] (%)	Flaming combustion time [b] (s)	Afterglow combustion time [c] (s)	Extinguishment	RMF [d] (%)
COT	-	53	-	NO	<1
COT/ DVP-CYSS	10	0	0	YES	100
COT/ M-CYSS	10	0	62	YES	90

[a] Add-on ± 0.5%. [b] Combustion time ± 1 s. [c] Combustion time ± 1 s. [d] RMF ± 1.0%

total heat release (THR) and residual mass fraction (RMF) are summarized in Table 5, while the corresponding HRR curves are displayed in Fig. 6.

Untreated cotton exhibited an intense flaming combustion, and after flameout, occurring at approximately 80 s, it was completely consumed due to pronounced afterglow. In contrast, at a 12.0% add-on, COT/DVP-CYSS burned more rapidly, resulting in a shorter TTI, but also reached TTF sooner (17 vs. 26 s and 49 vs. 78 s for COT/DVP-CYSS and COT, respectively), while showing a 24% reduction of cotton pkHRR and no evidence of afterglow. Notably, following flameout, combustion of COT/DVP-CYSS progressed slowly till the set end of the test (150 s), still without afterglow, and left a final RMF of about 9%, compared to < 1% for untreated cotton (Table 5).

In addition, the total smoke release during the initial non-flaming phase ($TSR_{(NFP)}$) and during the flaming phase ($TSR_{(FP)}$) was collected and reported in Table 5. DVP-CYSS coating significantly reduced the smoke released during cotton combustion in both the absence and presence of flame, as indicated by the $TSR_{(NFP)}$ and $TSR_{(FP)}$ values. As regard CO and CO_2 emissions, the yield values measured by the analyzers were negligible for both untreated and treated cotton fabric.

At the end of the tests, the residue of the COT/DVP-CYSS specimen was analyzed by FE-SEM. As observed in the residue after thermo-oxidation at 300 °C (Fig. 3c–e), as well as after VFSTs (Fig. 4c–e) and HFSTs (Fig. 5b–e), the fabric's texture remained largely intact (Fig. 6b–e). EDS analysis revealed a uniform distribution of carbon (C), oxygen (O), nitrogen (N), sulfur (S), and phosphorus (P), consistent with the chemical composition of DVP-CYSS (Fig. 6e–f).

3.4.4. Progression of char composition in COT/DVP-CYSS combustion

EDS analyses of combusted COT/DVP-CYSS samples, obtained through controlled oxidation at 300 °C, VFSTs, HFSTs, and oxygen-consumption cone calorimetry tests, consistently showed a uniform elemental distribution, including not only carbon and oxygen, but also sulfur and phosphorus. The elemental compositions of COT/DVP-CYSS chars obtained under varying combustion conditions are shown in Table 6. It should be noted that the data presented in this table were obtained from samples with 12.0% DVP-CYSS add-on, the same composition used in the combustion tests, except for the VFST entries, where a 10.0% add-on was used. This was necessary because the sample with a 12.0% add-on did not combust, and there was insufficient char to carry out the analysis. The comparison of the elemental composition obtained from EDS analysis of an COT/DVP-CYSS sample with the theoretical composition of uncombusted samples containing 10.0% and 12.0% add-on shows substantial agreement between experimental and theoretical values. The only notable exception is the carbon content (C %), which is known to be problematic to determine accurately, especially for porous samples, due to the low atomic number of carbon. Overall, the elemental composition after oxidation follows a similar trend across all samples. Carbon content (C%) increases substantially

Table 5
Combustion data of untreated and DVP-CYSS-treated cotton fabrics by oxygen-consumption cone calorimetry (35 kWm^{-2}).

Sample	TTI [a] (s)	TTF [b] (s)	pkHRR [c] ($kW•m^{-2}$) *(reduction, %)*	THR [d] ($kW•m^{-2}$)	$TSR_{(NFP)}$ [e] ($m^2•m^{-2}$)	$TSR_{(FP)}$ [f] ($m^2•m^{-2}$) *(reduction, %)*	RMF [g] (%)
COT	26 ± 4	78 ± 5	110 ± 6	3.80 ± 0.14	0	5.8 ± 1.7	1.14 ± 0.55
COT/DVP-CYSS	17 ± 2	49 ± 3	84 ± 4 *(24)*	3.62 ± 0.29	0.5 ± 0.2	2.1 ± 0.3 *(-63)*	8.95 ± 1.21

[a] TTI: Time to ignition. [b] TTI: Time to flameout. [c] pKHRR: Heat release rate peak. [d] THR: Total heat release. [e] $TSR_{(NFP)}$: Total smoke release during non-flaming phase. [f] $TSR_{(FP)}$: Total smoke release during flaming phase. [g] Residual mass fraction.

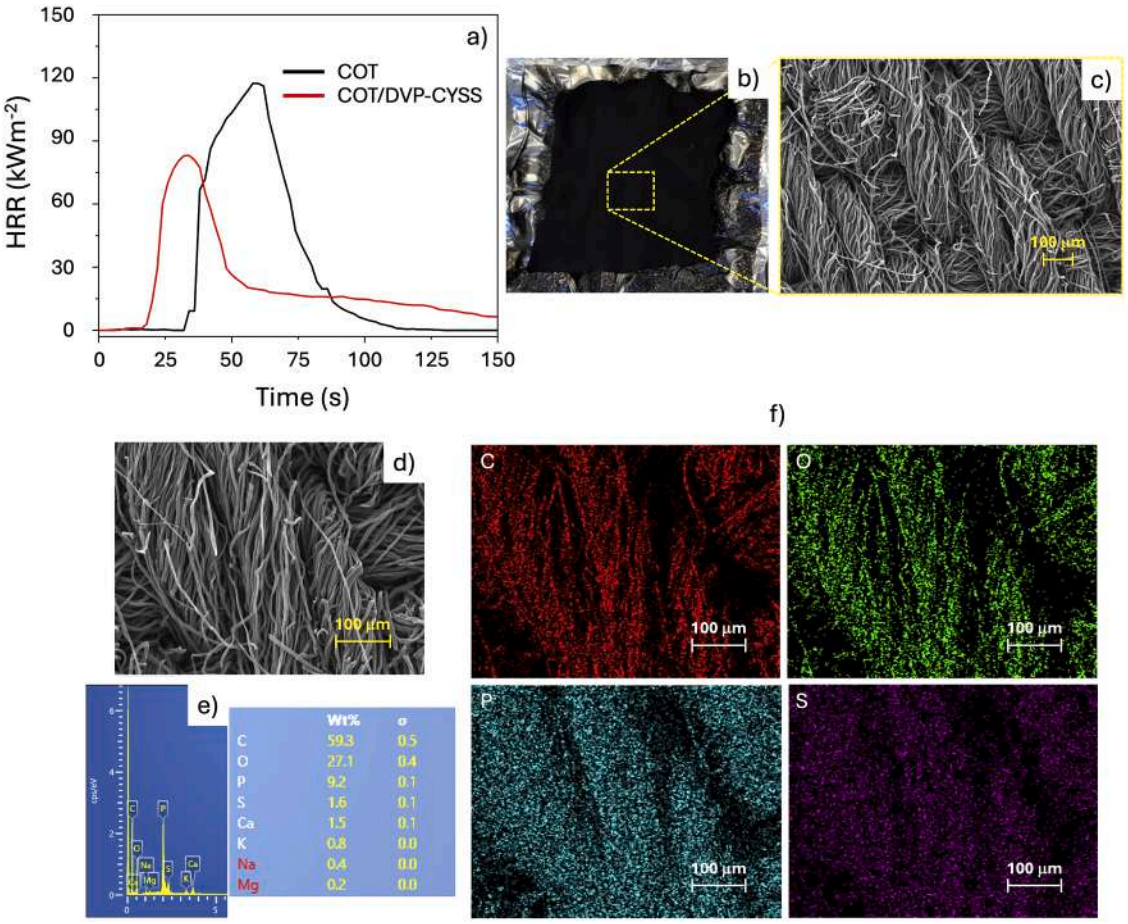

Fig. 6. HRR curves of untreated cotton (COT) and cotton treated with DVP-CYSS (COT/DVP-CYSS, add-on: 12.0%) obtained using an oxygen-consumption cone calorimeter under a heat flux of 35 kWm^{-2} (a). Digital image and SEM micrograph of COT/DVP-CYSS residue at the end of the test (b and c, 250x magnification). SEM micrograph (d, 500x magnification) and EDS analysis (e) with elemental maps of C (red), O (green), P (petrol blue), and S (purple) (f).

Table 6
COT/DVP-CYSS char composition under varying combustion conditions [(a)].

Sample origin	Add-on (%)	RMF [(b)] (%)	C%	O%	S%	P %
Theoretical values [(c, d)]	10	-	44	45.5	2.0	0.9
Theoretical values [(c, d)]	12	-	44	44.8	3.5	1.1
COT/DVP-CYSS	12	-	51.4	43.7	3.3	1.5
Combustion at 300 °C	12	55	53.4	42.4	2.0	1.6
VFSTs	10	65	71.6	22.0	1.8	3.9
Oxygen-consumption cone calorimetry	12	9.0	59.9	26.9	1.6	8.8
HFSTs	12	100	63.7	27.4	1.4	6.5

[(a)] Experimental values are the average of 5 independent measurements. [(b)] Residual mass fraction. [(c)] Uncombusted sample. [(d)] Theoretical values have been calculated considering the raw formula of the DVP-CYSS repeat unit, that is $C_{10}H_{23}N_2O_2PS_2$ (MM 298.40) and the theoretical add on (either 10.0 or 12.0%).

after combustion, reflecting both the loss of oxygen-containing functional groups, possibly due to decarboxylation and/or dehydration, evidenced by the decrease in O%, and aromatization, particularly pronounced in the VFST residue, which experienced the most severe combustion conditions. Simultaneously, sulfur content (S%) decreases, indicating the release of sulfur-containing fragments due to S–S bond cleavage and oxidation. In contrast, phosphorus content (P%) increases, demonstrating that phosphorus remains stably incorporated in the aromatic char.

4. Conclusions

This study demonstrated that the novel P/N/S-containing oligomer DVP-CYSS provides significantly improved flame retardant protection for cotton compared with the phosphorus-free S/N polyamidoamine M-CYSS. DVP-CYSS effectively suppressed combustion in both horizontal and vertical flame spread tests, achieving extinguishment at lower add-on levels and preventing ignition under conditions where M-CYSS-treated samples still burned and exhibited prolonged afterglow.

Oxygen-consumption cone calorimetry further confirmed the enhanced fire performance, with DVP-CYSS markedly reducing the main combustion parameters and increasing the residue mass fraction compared with untreated cotton. Analysis of the char composition indicated partial loss of sulfur due to disulfide bond cleavage and oxidation, whereas phosphorus remained largely in the residue, suggesting a predominant role in condensed-phase stabilization.

Overall, these results highlight the beneficial synergy among phosphorus, nitrogen, and sulfur in improving the flame retardancy of cotton, demonstrating the effectiveness of the DVP-CYSS oligomer as a multifunctional flame-retardant system.

It should be noted that the washing durability of DVP-CYSS is limited due to its high solubility in aqueous media. However, the performance observed in DVP-CYSS-impregnated cotton systems could be translated to chemically modified cotton via covalent grafting of DVP-CYSS or its analogues, representing a promising strategy to enhance treatment durability.

CRediT authorship contribution statement

Jenny Alongi: Writing – review & editing, Funding acquisition, Conceptualization. **Francesca Vasile:** Methodology, Investigation. **Federico Carosio:** Methodology, Investigation. **Matteo Arioli:** Investigation. **Domenico Albanese:** Writing – review & editing, Investigation, Conceptualization. **Elisabetta Ranucci:** Writing – original draft, Supervision, Conceptualization.

Declaration of competing interest

The authors declare that they have no known competing financial interests or personal relationships that could have appeared to influence the work reported in this paper.

Acknowledgments

The research was funded by Università degli Studi di Milano, Piano di Sostegno alla Ricerca 2023, Linea 2.

Supplementary materials

Supplementary material associated with this article can be found, in the online version, at doi:10.1016/j.polymdegradstab.2026.112059.

Data availability

The authors do not have permission to share data.

References

[1] R.A. Mensah, V. Shanmugam, S. Narayanan, J.S. Renner, K. Babu, R.E. Neisiany, M. Forsth, G. Sas, O. Das, A review of sustainable and environment-friendly flame retardants used in plastics, Polym. Test. 108 (2022) 107511, https://doi.org/10.1016/j.polymertesting.2022.107511.

[2] S. Shaw, Halogenated flame retardants: do the fire safety benefits justify the risks? Rev. Environ. Health 25 (2010) 261–305, https://doi.org/10.1515/REVEH.2010.25.4.261.

[3] H. Singh, A. Sivaramakrishna, Phosphorus-based polymeric flame retardants: recent advances and perspectives, Prog. Polym. Sci. 9 (2024) e202401485, https://doi.org/10.1002/slct.202401485.

[4] G. Camino, L. Costa, G. Martinasso, Intumescent fire-retardant systems, Polym. Degrad. Stab. 23 (1989) 359–376, https://doi.org/10.1016/0141-3910(89)90058-X.

[5] W. Tan, Y. Ren, M. Xiao, Y. Guo, Yansong Liu, J. Zhang, X. Zhou, X. Liu, Enhancing the flame retardancy of lyocell fabric finished with an efficient, halogen-free flame retardant, RSC Adv. 11 (2021) 34926–34937, https://doi.org/10.1039/D1RA06573D.

[6] M.S. Ozer, S. Gaan, Recent developments in phosphorus based flame retardant coatings for textiles: synthesis, applications and performance, Prog. Org. Coat. 171 (2022) 107027, https://doi.org/10.1016/j.porgcoat.2022.107027.

[7] Q. Yuan, S. Wang, L. He, S. Xu, Advances in the study of flame-retardant cellulose and its application in polymers: a review, Polymers 17 (2025) 1249, https://doi.org/10.3390/polym17091249.

[8] J. Alongi, E. Ranucci, Flame retardant applications of polyamidoamine dendrimers (PAMAM) and linear polyamidoamines (PAAs) in plastics and textiles, Polym. Degrad. Stabil. 241 (2025) 111516, https://doi.org/10.1016/j.polymdegradstab.2025.111516.

[9] A. Battig, J.C. Markwart, F.R. Wurm, B. Schartel, Sulfur's role in the flame retardancy of thio-ether–linked hyperbranched polyphosphoesters in epoxy resins, Eur. Polym. J. 122 (2020) 109390, https://doi.org/10.1016/j.eurpolymj.2019.109390.

[10] W. Pawelec, A. Holappa, T. Tirri, M. Aubert, H. Hoppe, R. Pfaendner, C.-E. Wilén, Disulfides - Effective radical generators for flame retardancy of polypropylene, Polym. Degrad. Stabil. 110 (2014) 447, https://doi.org/10.1016/j.polymdegradstab.2014.09.013, e456.

[11] W. Jiang, F.L. Jin, S.J. Park, Synthesis of a novel phosphorus-nitrogen-containing intumescent flame retardant and its application to fabrics, J. Ind. Eng. Chem. 27 (2015) 40–43, https://doi.org/10.1016/j.jiec.2015.01.010.

[12] T.-M. Nguyen, S. Chang, B. Condon, R. Slopek, E. Graves, M. Yoshioka-Tarver, Structural effect of phosphoramidate derivatives on the thermal and flame retardant behaviors of treated cotton cellulose, Ind. Eng. Chem. Res. 52 (2013) 4715–4724, https://doi.org/10.1021/ie400180f.

[13] K. Dai, Z. Deng, G. Liu, Y. Wu, W. Xu, Y. Hu, Effects of a reactive phosphorus–sulfur containing flame-retardant monomer on the flame retardancy and thermal and mechanical properties of unsaturated polyester resin, Polymers 12 (2020) 1441, https://doi.org/10.3390/polym12071441.

[14] S. Chang. M. Nguyen, B.D: Condon, J. Smith, The comparison of phosphorus-nitrogen and sulfur-phosphorus-nitrogen on the anti-flammability and thermal degradation of cotton fabrics, Fibers Polym. 18 (2017) 666–674, https://doi.org/10.1007/s12221-017-6686-x.

[15] Z. Jiang, Z. Chen, Z. Luo, B. Wang, A P/N/S containing flame retardant for epoxy resins with excellent optical, mechanical and flame retardant properties, Polym. Degrad. Stabil. 225 (2024) 110783, https://doi.org/10.1016/j.polymdegradstab.2024.110783.

[16] Y. Wang, L. Ma, J. Yuan, Z. Zhu, X. Liu, D. Li, L. He, F. Xiao, Furfural-based P/N/S flame retardant towards high-performance epoxy resins with flame retardancy, toughness, low dielectric properties and UV resistance, Polym. Degrad. Stabil. 212 (2023) 110343, https://doi.org/10.1016/j.polymdegradstab.2023.110343.

[17] A. Beduini, D. Albanese, F. Carosio, A. Manfredi, E. Ranucci, P. Ferruti, J. Alongi, On the suitability of phosphonate-containing polyamidoamines as cotton flame retardants, Polymers 15 (2023) 1869, https://doi.org/10.3390/polym15081869.

[18] A. Manfredi, F. Carosio, P. Ferruti, J. Alongi, E. Ranucci, Disulfide-containing polyamidoamines with remarkable flame retardant activity for cotton fabrics, Polym. Degrad. Stabil. 156 (2018) 1–13, https://doi.org/10.1016/j.polymdegradstab.2018.07.028.

[19] A. Beduini, P. Ferruti, F. Carosio, E. Ranucci, J. Alongi, Sulfur-based copolymeric polyamidoamines as efficient flame-retardants for cotton, Polymers 11 (2019) 1904, https://doi.org/10.3390/polym11111904.

[20] A.-P. Schaffner, P. Sansilvestri-Morel, N. Despaux, E. Ruano, T. Persigand, A. Rupin, P. Mennecier, M.-O. Vallez, E. Raimbaud, P. Desos, P. Gloanec, Phosphinanes and azaphosphinanes as potent and selective inhibitors of activated thrombin-activatable fibrinolysis inhibitor (TAFIa), J. Med. Chem. 64 (2021) 3897–3910, https://doi.org/10.1021/acs.jmedchem.0c02072.

[21] M. Si, J. Feng, J. Hao, L. Xu, J. Du, Synergistic flame retardant effects and mechanisms of nano-Sb_2O_3 in combination with aluminum phosphinate in pol (ethyene terephthalate), Polym. Degrad. Stab. 100 (2014) 70–78, https://doi.org/10.1016/j.polymdegradstab.2013.12.023.

[22] U. Braun, B. Schartel, M.A. Fichera, C. Jäger, Flame retardancy mechanisms of aluminium phosphinate in glass-fibre reinforced polyamide 6,6, Polym. Degrad. Stab. 92 (2007) 1528–1545, https://doi.org/10.1016/j.polymdegradstab.2007.05.007.

[23] S.V. Levchik, E.D. Weil, A review of recent progress in phosphorus-based flame retardants, J. Fire Sci. 24 (2006) 345–364, https://doi.org/10.1177/0734904106068426.

[24] B. Schartel, Phosphorus-based flame retardancy mechanisms—old hat or a starting point for future development? Materials 9 (2016) 1–25, https://doi.org/10.3390/ma3104710.

[25] Q. Yao, Y. Zhang, X. Wang, Synthesis and application of hybrid aluminum dialkylphosphinates as flame retardants for poly-amides, Polymers 15 (2023) 4612, https://doi.org/10.3390/polym15234612.

[26] J. Wagner, P. Deglmann, S. Fuchs, M. Ciesielski, C.A. Fleckenstein, M. Döring, A flame retardant synergism of organic disulfides and phosphorous compounds, Polym. Degrad. Stabil. 129 (2016) 63–76.

[27] M. Banks, J.R. Ebdon, M. Johnson, A flame retardant synergism of organic disulfides and phosphorous compounds, Polymer 35 (1994) 3470–3473, https://doi.org/10.1016/j.polymdegradstab.2016.03.023.

[28] J. Alongi, P. Ferruti, A. Manfredi, F. Carosio, Z. Feng, M. Hakkarainen, E. Ranucci, Superior flame retardancy of cotton by synergetic effect of cellulose-derived nano-graphene oxide carbon dots and disulphide-containing polyamidoamines, Polym. Degrad. Stab. 169 (2019) 108993, https://doi.org/10.1016/j.polymdegradstab.2019.108993.

[29] ISO 2469 Paper, Board and Pulps - Measurement of Diffuse Radiance Factor (Diffuse Reflectance Factor), International Organization for Standardization, Geneve, Switzerland, 2024.

[30] ISO 13934-1, Textile - Tensile Properties of Fabrics. Part 1: Determination of Maximum Force and Elongation at Maximum Force Using the Strip Method, International Organization for Standardization, Geneve, Switzerland, 2013.

[31] ISO 3795, Road Vehicles, and Tractors and Machinery for Agriculture and Forestry - Determination of Burning Behaviour of Interior Materials, International Organization for Standardization, Geneve, Switzerland, 2019.

[32] ISO 15025, Protective Clothing - Protection Against Flame - Method of Test for Limited Flame Spread, International Organization for Standardization, Geneve, Switzerland, 2016.

[33] J. Tata, J. Alongi, F. Carosio, A. Frache, Optimization of the procedure to burn textile fabrics by cone calorimeter: Part I, Combustion Behavior of Polyester, Fire Mater 35 (2011) 397–409, https://doi.org/10.1002/fam.1061.

[34] ISO 5660, Fire Test. Reaction to Fire, Rate of Heat Release - Cone Calorimeter Method, International Organization for Standardization, Geneva, Switzerland, 2002.

[35] S. Viel, Diffusion-ordered NMR spectroscopy: a versatile tool for the molecular weight determination of uncharged polysaccharides, Biomacromolecules 4 (2003) 1843–1847, https://doi.org/10.1021/bm0342638.

[36] E. Ranucci, J. Alongi, Thermal decomposition of cellulosic materials: insights into mechanisms and product evolution, Polym. Degrad. Stabil. 242 (2025) 111629, https://doi.org/10.1016/j.polymdegradstab.2025.111629.